Salvaging the Overlooked: Leveraging Class-Aware Contrastive Learning for Multi-Class Anomaly Detection

Supplementary material

Lei Fan[1*] Junjie Huang[2] Donglin Di[2] Anyang Su[2]
Tianyou Song[3] Maurice Pagnucco[1] Yang Song[1]
[1]UNSW Sydney [2]DZ-Matrix [3]Columbia University
https://lgc-ad.github.io/

In this supplementary material, we provide a detailed overview of the model architecture and experimental settings. This document includes:

- A comprehensive description of the model architecture and the pseudo-code for computing local CL and global CL, as presented in Section 1.
- Detailed experimental results corresponding to Figure 1a and Table 4, as provided in Section 2.
- Detailed experimental settings for multi-class and reconstruction-based models, as outlined in Section 3.

1. Model Architecture

We provided detailed architecture in Figure I and Python-style pseudo-code for computing local CL and global CL in Code 1. Specifically,

- The encoder employs a pretrained WideResNet50 [6], extracting features from the first three residual blocks, denoted as $\mathcal{R}_e^1$, $\mathcal{R}_e^2$, and $\mathcal{R}_e^3$.
- The projector employs a convolutional block with $N = 4$.
- The neck utilizes convolutional layers to align multi-scale features using a 1×1 convolution layers.
- The decoder adopts a symmetrical structure to the encoder, utilizing the first three residual blocks of a randomly initialized WideResNet50, denoted as $\mathcal{R}_d^1$, $\mathcal{R}_d^2$, and $\mathcal{R}_d^3$. Deconvolution layers with a kernel size of 2×2 are applied before each block to upsample the features.

2. Detailed Results

We provided specific experimental results across multiple comparison experiments:

- Table I provides detailed results corresponding to **Figure 1.(a)**, using various one-for-all training strategies to enhance previously one-for-one models [2, 21] on four datasets [1, 13, 17, 22]. Detailed results are reported in terms of I/P-AUROC for each category.

*Corresponding author: lei.fan1@unsw.edu.au

```python
# pretrained encoder:f_e, decoder:f_d, neck:f_n, projector:f_p
for x, raw_class in data_loader:
 x_aug = aug(x)  # data augmentation

 # extracting multi-scale features
 z_e = f_e.forward(x)
 z_e_aug = f_e.forward(x_aug)

 # projector
 z_p = f_p.forward(z_e)
 z_p_aug = f_p.forward(z_e_aug)

 # bottle neck
 z_n = f_n.forward(z_p)
 z_n_aug = f_n.forward(z_p_aug)

 # compute local CL
 local_index = find_local_similarity_index(z_p, z_p_aug, label)
 loss_lcl = local_cl(z_p, z_p_aug, local_index, label)

 # compute global CL
 loss_gcl = global_cl(z_n, z_n_aug, label)


 z_d = f_d.forward(z_n)  # features reconstruction for decoder

 # compute knowledge distillation loss
 loss_kd = cosine_similarity(z_e, z_d)

 # compute total loss
 loss = lambda_1 * loss_lcl + lambda_2 * loss_gcl + loss_kd

 loss.backward()
 update(f_d, f_n, f_p)
```

Code 1. Pseudo-code for local CL and global CL.

- Table II presents detailed results corresponding to **Table 4**, using various one-for-all training strategies to enhance previously one-for-one models [2, 10, 19, 21] on three datasets [1, 13, 22]. Data from these three datasets are mixed for the multi-class setting, and results are reported in terms of I-/P-AUROC for each category.

3. Implementation Details

3.1. Multi-class Models

We provided detailed experimental settings of various multi-class models for **Table 1** and **Table 4**. Typically, we leveraged the official code for each method to evaluate the models.

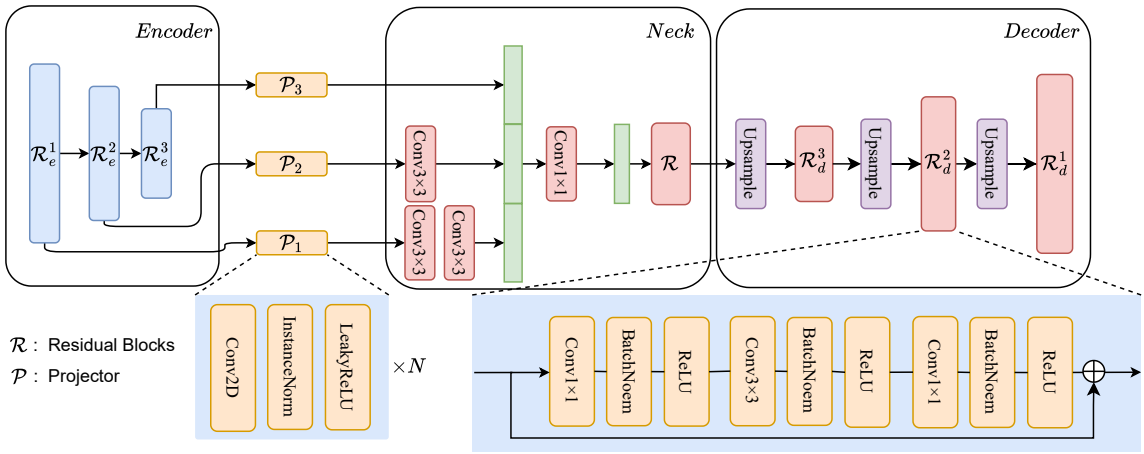

Figure I. The detailed architecture of RD [2] with our LGC training strategy.

- UniAD [18]: The model was trained for 1000 epochs with a batch size of 64. The input image size was set to 256 × 256. The optimizer was AdamW [12], configured with $\beta_1 = 0.9$, $\beta_2 = 0.999$, and a weight decay of 1×10^{-4}. The learning rate was set to 1×10^{-4}, and the loss function was FeatureMSELoss. The backbone network used was EfficientNet-B4 [16].
- CRAD [9]: The model was trained for 50 epochs with a batch size of 16, and the input image size was set to 224 × 224. The optimizer was AdamW [12], with a learning rate of 0.1 for the grid parameters and 0.001 for the network parameters. The learning rate scheduler was StepLR, configured with a step size of 40 and a decay factor (γ) of 0.1. The loss function was FeatureMSELoss, and the backbone was EfficientNet-B4 [16].
- OneNIP [3]: The model was trained for 1000 epochs with a batch size of 8, and the input image size was set to 224 × 224. The optimizer was AdamW [12], configured with $\beta_1 = 0.9$, $\beta_2 = 0.999$, and a weight decay of 1×10^{-4}. The learning rate was set to 1×10^{-4}, with a StepLR scheduler using a step size of 800 and a decay factor (γ) of 0.1. The loss function was FeatureMSELoss, and the backbone was EfficientNet-B4 [16].
- DiAD [4]: The model was trained for 1000 epochs with a batch size of 12, and the input image size was set to 256 × 256. The optimizer was AdamW [12], with a learning rate of 1×10^{-5}. The loss function was DDPM [7], and the backbone was Stable Diffusion 1.5 [14].
- MambaAD [5]: The model was trained for 1000 epochs with a batch size of 16, and the input image size was set to 256 × 256. The optimizer was AdamW [12], configured with $\beta_1 = 0.9$, $\beta_2 = 0.999$, and a weight decay of 1×10^{-4}. The learning rate was set to 0.005, and the loss function was MSE Loss. The backbone used was ResNet34 [6].
- ViTAD [20]: The model was trained for 100 epochs with a batch size of 8, and the input image size was set to 256 × 256. The optimizer was AdamW [12], configured with $\beta_1 = 0.9$, $\beta_2 = 0.999$, and a weight decay of 1×10^{-4}. The learning rate was set to 0.0001.

3.2. Reconstruction-based Models

We provided detailed experimental settings of various reconstruction-class models for **Figure 1a** and **Table 4**. Typically, we leveraged the official code for each method to evaluate the models.

- DeSTSeg [21]: It consists of two training stages. The model was trained for 40 epochs with a batch size of 32 and an image size of 256 × 256. The optimizer was SGD with a learning rate of 0.4 and a momentum of 0.9. The loss function was Cosine Similarity, and the backbone network was ResNet18 [6]. Then, the training continued for 160 epochs, but separate learning rates were applied: 0.1 for the backbone and 0.01 for the head. The loss functions were L1 Loss and Focal Loss [15].
- DRAEM [19]: The model was trained for 200 epochs with a batch size of 8 and an image size of 256 × 256. The optimizer used is Adam [8], configured with $\beta_1 = 0.5$ and $\beta_2 = 0.999$. The learning rate was set to 1×10^{-4}. The loss functions included L2 loss and SSIM loss for reconstruction, and Focal Loss [15] for discrimination tasks.
- DMAD [10]: We employed the DDPM version. The model was trained for 200 epochs with a batch size of 16 and an image size of 256 × 256. The optimizer was Adam [8]. The learning rate was set to 0.005. The loss function was based on Cosine Similarity, and the backbone was WideResNet50 [6].
- CRD [11]: The model was trained for 200 epochs with a batch size of 16, and the input size was set to 256 × 256. The optimizer was Adam, configured with $\beta_1 = 0.9$,

$\beta_2 = 0.999$, and a weight decay of 0.95. The learning rate was set to 0.005.

References

[1] Paul Bergmann, Michael Fauser, David Sattlegger, and Carsten Steger. MVTec AD–A comprehensive real-world dataset for unsupervised anomaly detection. In *CVPR*, pages 9592–9600, 2019.

[2] Hanqiu Deng and Xingyu Li. Anomaly detection via reverse distillation from one-class embedding. In *CVPR*, pages 9737–9746, 2022.

[3] Bin-Bin Gao. Learning to detect multi-class anomalies with just one normal image prompt. In *ECCV*, 2024.

[4] Haoyang He, Jiangning Zhang, Hongxu Chen, et al. A diffusion-based framework for multi-class anomaly detection. In *AAAI*, pages 8472–8480, 2024.

[5] Haoyang He, Yuhu Bai, Jiangning Zhang, et al. MambaAD: Exploring state space models for multi-class unsupervised anomaly detection. *NeurIPS*, 37:71162–71187, 2025.

[6] Kaiming He, Xiangyu Zhang, Shaoqing Ren, and Jian Sun. Deep residual learning for image recognition. In *CVPR*, pages 770–778, 2016.

[7] Jonathan Ho, Ajay Jain, and Pieter Abbeel. Denoising diffusion probabilistic models. *NeurIPS*, 33:6840–6851, 2020.

[8] Diederik P Kingma. Adam: A method for stochastic optimization. *arXiv preprint arXiv:1412.6980*, 2014.

[9] Joo Chan Lee, Taejune Kim, Eunbyung Park, Simon S. Woo, and Jong Hwan Ko. Continuous memory representation for anomaly detection. *ECCV*, 2024.

[10] Wenrui Liu, Hong Chang, Bingpeng Ma, Shiguang Shan, and Xilin Chen. Diversity-measurable anomaly detection. In *CVPR*, pages 12147–12156, 2023.

[11] Xinyue Liu, Jianyuan Wang, Biao Leng, and Shuo Zhang. Multimodal industrial anomaly detection by crossmodal reverse distillation. *preprint arXiv:2412.08949*, 2024.

[12] I Loshchilov. Decoupled weight decay regularization. *arXiv preprint arXiv:1711.05101*, 2017.

[13] Pankaj Mishra, Riccardo Verk, Daniele Fornasier, et al. VT-ADL: A vision transformer network for image anomaly detection and localization. In *International Symposium on Industrial Electronics*, pages 01–06, 2021.

[14] Robin Rombach, Andreas Blattmann, Dominik Lorenz, Patrick Esser, and Björn Ommer. High-resolution image synthesis with latent diffusion models. In *CVPR*, pages 10684–10695, 2022.

[15] T-YLPG Ross and GKHP Dollár. Focal loss for dense object detection. In *CVPR*, pages 2980–2988, 2017.

[16] Mingxing Tan and Quoc Le. Efficientnet: Rethinking model scaling for convolutional neural networks. In *ICML*, pages 6105–6114. PMLR, 2019.

[17] Chengjie Wang, Wenbing Zhu, Bin-Bin Gao, et al. Real-iad: A real-world multi-view dataset for benchmarking versatile industrial anomaly detection. In *CVPR*, pages 22883–22892, 2024.

[18] Zhiyuan You, Lei Cui, Yujun Shen, Kai Yang, Xin Lu, Yu Zheng, and Xinyi Le. A unified model for multi-class anomaly detection. *NeurIPS*, 35:4571–4584, 2022.

[19] Vitjan Zavrtanik, Matej Kristan, and Danijel Skočaj. Draema discriminatively trained reconstruction embedding for surface anomaly detection. In *ICCV*, pages 8330–8339, 2021.

[20] Jiangning Zhang, Xuhai Chen, Yabiao Wang, Chengjie Wang, Yong Liu, Xiangtai Li, Ming-Hsuan Yang, and Dacheng Tao. Exploring plain vit reconstruction for multi-class unsupervised anomaly detection. *Computer Vision and Image Understanding*, 2025.

[21] Xuan Zhang, Shiyu Li, Xi Li, Ping Huang, Jiulong Shan, and Ting Chen. Destseg: Segmentation guided denoising student-teacher for anomaly detection. In *CVPR*, pages 3914–3923, 2023.

[22] Yang Zou, Jongheon Jeong, Latha Pemula, Dongqing Zhang, and Onkar Dabeer. Spot-the-difference self-supervised pre-training for anomaly detection and segmentation. In *ECCV*, pages 392–408. Springer, 2022.

Table I. **Detailed results for Figure 1a**. The evaluation of one-for-one models: RD [2] and DeSTSeg [21] through four one-for-all training strategies: Sequential, Continual, Joint, and LGC. Results are reported as I/P-AUROC (%). The results obtained using separate models for each category are presented in the *One4one* columns, while *total average* is computed based on four dataset averages.

	Dataset	RD [2]					DeSTSeg [21]				
		One4one	Sequential	Continual	Joint	LGC(our)	*One4one*	Sequential	Continual	Joint	LGC(our)
MVTec AD [1]	bottle	100/98.7	84.8/80.0	69.8/78.5	97.7/99.6	100/98.2	100/99.2	41.7/67.0	48.7/63.9	100.0/96.9	100.0/97.3
	cable	95.0/97.4	57.0/61.2	61.3/60.5	82.3/94.7	99.5/98.2	97.8/97.3	46.2/60.9	47.7/53.0	93.9/93.7	95.8/95.1
	capsule	96.3/98.7	67.0/94.6	65.2/93.5	97.6/85.3	97.2/96.8	97.0/99.1	58.1/87.7	55.9/83.5	91.5/93.5	96.0/91.9
	carpet	98.9/98.9	83.0/96.5	90.0/97.5	99.0/99.2	98.9/99.0	98.9/96.1	85.0/81.5	88.0/58.4	99.0/95.9	98.4/97.4
	grid	100/99.3	61.5/76.5	55.6/67.4	98.3/98.7	98.4/99.2	99.7/99.1	48.9/47.8	50.0/51.6	100.0/97.0	100.0/99.2
	hazelnut	99.9/98.9	87.0/96.9	93.7/96.3	99.0/100.0	100/99.0	99.9/99.6	40.8/83.6	49.8/83.3	100.0/96.2	100.0/96.0
	leather	100/99.4	58.9/92.6	68.0/95.5	99.4/100.0	100/99.5	100/99.7	60.9/56.2	74.7/52.9	100.0/99.4	100.0/99.7
	metal_nut	100/97.3	68.4/81.8	97.8/93.3	95.8/99.7	100/97.6	99.5/98.6	52.3/76.6	63.0/75.1	100.0/96.6	100.0/97.4
	pill	96.6/98.2	98.1/97.8	90.7/95.2	96.9/91.8	98.4/98.9	97.2/98.7	95.9/89.6	95.9/96.0	92.4/95.1	94.2/93.6
	screw	97.0/99.6	99.1/99.5	82.1/97.8	98.6/86.7	97.4/99.1	93.6/98.5	91.9/85.3	92.8/82.8	84.6/88.4	90.3/85.5
	tile	99.3/95.6	72.9/77.4	82.1/79.4	95.3/99.6	99.8/97.1	100/98.0	82.7/55.2	69.1/50.7	100.0/98.6	100.0/98.4
	transistor	96.7/92.5	91.1/99.1	86.9/99.1	99.0/99.4	99.6/95.5	98.5/89.1	92.8/97.7	98.9/98.8	90.0/98.4	94.4/98.7
	troothbrush	99.5/99.1	94.7/86.5	94.3/86.5	85.5/94.1	100/99.2	99.9/99.3	98.7/82.6	99.0/85.6	98.2/75.2	96.0/79.4
	wood	99.2/95.3	89.4/89.1	88.7/89.4	95.3/99.0	99.9/96.9	97.1/97.7	49.1/63.8	63.8/50.9	99.6/94.6	99.6/95.1
	zipper	98.5/98.2	66.9/97.5	99.2/98.2	97.2/99.4	99.8/97.8	100/99.1	99.7/91.9	97.7/86.0	99.7/95.1	99.8/95.7
	average	98.5/97.8	78.7/88.5	81.7/88.5	96.5/95.8	99.3/98.2	98.6/97.9	69.6/75.2	73.0/71.5	95.6/92.9	97.6/94.7
VisA [22]	candle	95.1/98.9	59.0/91.5	71.4/91.8	92.5/99.2	97.6/99.1	96.2/89.6	51.9/65.9	47.4/82.6	88.5/85.2	94.2/91.4
	capsules	89.4/99.6	47.8/81.3	47.2/80.2	83.8/99.4	86.0/99.4	86.9/96.5	60.8/64.0	38.8/70.5	85.9/95.0	92.4/97.1
	cashew	96.7/95.5	95.5/91.5	95.8/93.1	94.3/92.3	96.9/94.2	94.2/96.3	84.1/89.8	90.6/81.3	90.3/90.9	92.2/91.2
	chewinggum	98.1/98.8	97.4/98.7	97.7/98.9	96.4/98.8	97.9/97.5	98.2/97.4	97.2/97.7	97.7/98.9	96.1/98.4	97.4/98.7
	fryum	95.5/96.5	96.9/96.7	97.1/96.8	95.9/96.9	95.9/97.3	88.6/89.2	93.4/74.2	95.2/71.9	91.4/67.9	94.6/75.7
	macaroni1	93.7/99.6	54.7/95.3	47.3/95.3	95.8/99.8	98.3/99.4	94.9/97.5	48.8/73.6	44.7/84.9	94.1/90.2	93.9/96.2
	macaroni2	87.2/99.5	41.0/94.2	48.4/94.6	87.7/99.6	85.8/99.3	80/92	56.2/87.8	50.4/92.0	73.7/76.0	74.2/83.5
	pcb1	96.5/99.7	59.5/78.6	63.1/78.4	96.7/99.5	98.4/99.6	96/94.6	35.3/67.1	78.0/66.3	90.8/98.0	93.6/98.7
	pcb2	97.3/98.9	66.2/82.8	62.3/83.4	97.8/98.0	96.9/98.8	96.5/95.4	48.1/70.6	51.3/82.3	93.2/97.6	95.1/97.2
	pcb3	97.1/99.2	55.7/85.5	52.3/85.8	96.7/98.1	96.8/99.1	97.8/94.1	49.1/82.4	48.3/84.6	96.4/94.1	96.5/93.9
	pcb4	99.8/98.4	28.0/77.5	29.0/77.8	100.0/97.8	100.0/98.6	99.5/92.4	68.6/82.2	76.6/80.6	99.1/92.8	99.2/95.0
	pipe_fryum	99.6/98.9	99.1/99.0	98.7/99.0	98.0/99.1	99.1/99.3	98.8/89.9	98.8/95.2	99.1/94.1	98.2/94.6	98.4/95.2
	avgerage	95.5/98.6	66.7/89.4	67.5/89.6	93.6/98.2	95.9/98.5	93.9/93.7	66.0/79.2	68.2/82.5	91.5/90.1	92.8/91.6
BTAD [13]	01	99.7/97.6	74.6/88.2	83.3/86.2	99.8/97.7	100.0/97.7	98.4/92.4	42.9/58.5	43.9/56.6	97.3/92.8	98.9/91.5
	02	84.7/96.7	80.5/93.7	82.1/92.7	84.9/96.6	87.8/96.6	84/92.9	35.8/52.0	64.9/65.9	84.3/91.1	85.6/92.7
	03	99.4/99.7	98.4/98.7	99.2/98.7	99.6/99.7	99.7/99.7	99.1/98.8	99.5/98.8	99.6/98.8	99.4/98.5	99.5/98.4
	average	94.6/98.0	84.5/93.5	88.2/92.5	94.8/98.0	95.7/98.0	93.8/94.7	59.4/69.8	69.5/73.8	93.7/94.1	94.7/94.3
Real-IAD [17]	audoijack	83.5/91.2	54.2/93.1	54.4/93.2	68.7/94.0	81.6/97.7	81.5/93.9	43.8/86.9	51.0/89.4	81.2/89.8	83.5/91.4
	bottle_cap	90.5/92.6	71.2/97.3	71.7/97.5	81.2/98.9	90.2/99.5	91.8/97.4	61.5/84.9	48.5/84.3	85.7/80.8	89.1/86.5
	button_battery	83.6/94.1	58.9/93.9	63.0/93.8	65.4/95.8	81.0/98.7	92.3/94.3	46.7/87.5	52.1/88.9	88.8/91.8	86.9/93.1
	end_cap	69.7/91.2	55.0/88.4	54.1/88.9	69.1/93.7	81.8/97.3	86.5/84.9	50.8/74.2	51.3/77.3	79.6/76.7	79.9/80.0
	eraser	87.5/95.4	83.1/99.1	82.8/99.1	84.7/99.2	90.8/99.2	90.5/96.6	72.7/82.6	65.7/92.2	83.9/87.8	83.1/92.2
	fire_hood	92.5/96.9	75.4/97.6	75.5/97.6	78.6/98.1	81.0/98.5	83.3/93.5	64.0/77.9	71.6/89.7	82.4/90.8	82.5/91.6
	mint	63.6/78.3	51.9/85.5	51.8/86.1	59.9/91.6	73.6/96.8	74.2/85.9	53.7/75.9	53.5/79.9	63.9/73.6	63.5/73.5
	mounts	91.1/98.1	72.7/95.7	73.2/96.1	82.5/98.5	89.8/99.3	84.2/92.2	49.6/82.5	50.4/85.0	78.0/88.7	78.7/89.9
	pcb	89.6/93.8	53.8/89.5	53.6/89.7	72.9/95.5	91.8/99.2	90.3/94.4	41.8/88.0	42.5/89.0	84.3/92.8	84.8/91.1
	phone_battery	90.4/94.7	53.4/72.0	54.8/72.8	77.6/79.8	92.8/98.9	87.4/93.8	56.1/73.8	55.7/76.9	84.8/76.8	86.8/79.5
	plastic_nut	82.6/93.2	63.5/91.2	62.1/91.2	73.0/96.3	87.8/99.4	91.4/96.7	52.2/69.6	48.4/71.6	84.0/88.8	85.0/88.8
	plastic_plug	90.9/97.2	46.0/89.6	45.8/91.0	73.2/98.0	88.7/98.7	86.4/89.5	56.5/81.9	58.3/79.8	78.8/77.7	80.2/75.8
	porcelain_doll	87.5/95.4	75.0/93.9	73.1/94.4	84.7/98.6	88.5/98.6	84.5/87.9	51.4/88.5	57.9/79.6	74.5/70.7	78.2/79.1
	regulator	87.8/98.9	59.0/86.2	58.5/86.7	58.2/94.1	75.2/98.8	92/92.1	51.4/76.0	59.2/76.9	78.2/78.7	81.3/81.0
	rolled_strip_base	94.9/96.1	71.2/95.6	73.9/96.1	93.7/99.3	99.4/99.6	98.6/97.6	52.7/86.1	49.9/88.5	97.5/95.9	96.2/95.7
	sim_card_set	91.9/97.3	70.9/96.0	69.3/96.2	90.5/98.1	96.5/97.5	92.5/97.1	43.5/86.1	40.2/84.4	93.7/97.9	93.9/96.8
	switch	91.8/93.7	53.4/82.7	53.5/82.9	76.1/89.8	93.8/98.6	93.7/97.9	50.5/77.4	48.7/74.0	90.8/90.9	91.0/88.7
	tape	98.2/98.8	82.7/98.3	82.7/98.3	93.7/99.5	96.5/99.6	96.3/97.6	44.7/70.9	51.2/79.9	95.6/94.9	95.8/95.4
	terminalblock	97.4/98.8	52.0/93.8	53.6/94.1	78.9/98.8	94.1/99.7	94.8/97.8	44.2/85.6	47.4/86.5	90.9/93.9	91.7/95.0
	toothbrush	85.6/95.3	61.5/94.3	65.7/94.6	76.9/95.0	87.9/97.7	89.6/88.6	55.9/90.1	55.1/91.3	84.7/79.8	81.0/83.0
	toy	86.6/93.9	75.2/95.9	74.3/96.0	60.2/90.8	82.6/96.9	84.2/79.3	76.0/63.2	76.6/69.6	76.9/75.7	76.5/76.6
	toy_brick	82.1/90.1	67.0/96.6	65.6/96.5	59.8/93.9	69.7/96.4	82.5/88.4	75.3/77.3	74.6/84.0	73.4/83.7	75.2/87.2
	transistor1	93.5/96.5	94.3/99.3	94.9/99.3	82.3/97.8	97.0/99.5	96.3/97.8	94.6/88.9	92.5/91.7	89.7/90.8	91.5/92.1
	u_block	88.5/98.1	90.9/99.5	91.2/99.5	84.0/99.3	90.4/99.5	90.1/90.7	84.0/84.9	83.7/92.2	83.8/89.8	88.1/94.0
	usb	88.5/98.0	88.2/98.6	88.8/98.6	71.3/95.2	94.2/99.4	91.6/97.5	91.4/92.5	90.4/94.3	88.8/92.8	90.1/95.4
	usb_adapter	78.8/91.3	74.5/95.0	74.7/94.9	65.2/92.9	80.5/96.1	78.1/93	82.4/80.0	80.3/85.7	83.1/86.8	82.7/84.7
	vcpill	90.6/94.9	87.0/98.3	87.0/98.3	79.6/96.3	87.5/98.2	89.6/92.3	81.0/70.1	79.9/86.1	79.1/83.7	82.0/85.3
	wooden_beads	78.8/85.6	82.4/97.9	82.7/97.9	78.1/97.0	86.8/97.9	87/91.3	85.0/79.9	84.0/90.0	83.5/86.8	84.8/90.0
	woodstick	89.4/94.9	79.6/98.0	78.6/97.9	76.4/96.9	77.9/97.9	87.4/95.3	82.9/90.3	81.4/91.5	82.9/92.8	83.2/92.0
	zipper	99.6/98.1	97.4/99.2	97.6/99.2	97.6/98.8	99.1/99.3	97.9/84.7	96.5/73.7	97.0/79.9	97.4/87.9	96.2/90.8
	average	87.6/94.4	70.0/93.7	70.3/93.9	76.4/95.7	87.6/98.5	88.9/92.5	63.1/80.9	63.3/84.3	82.3/85.8	84.8/87.9
total average		94.0/97.2	74.9/91.3	76.9/91.4	90.3/96.9	94.6/98.3	93.8/94.7	64.5/76.3	68.5/78.0	90.7/90.9	92.5/92.3

Table II. **The detailed results for Table 4**. The evaluation of one-for-one models: DRAEM [19], DMAD [10], RD [2] and DeSTSeg [21] through two one-for-all training strategies: Joint and LGC. Results are reported as I/P-AUROC (%). The results obtained using separate models for each category are presented in the *One4one* columns, while *total average* is computed based on all categories. To enhance clarity, we omitted the PRO metric which can be found in detail on the project homepage.

	Dataset	DRAEM [19]			DMAD [10]			RD [2]			DeSTSeg [21]		
		One4one	Joint	LGC(our)	*One4one*	Joint	LGC(our)	*One4one*	Joint	LGC(our)	*One4one*	Joint	LGC(our)
MVTec AD [1]	bottle	99.2/99.1	99.1/85.0	98.1/96.1	100/98.9	98.6/97.6	99.7/98.3	98.6/99.0	98.6/99.0	98.4/99.0	100/99.2	99.9/92.3	99.9/96.0
	cable	91.8/94.7	59.4/71.7	64.1/68.5	99.1/98.1	78.8/83.3	95.4/95.7	98.9/97.2	98.9/97.2	100.0/98.4	97.8/97.3	88.2/76.7	94.2/86.8
	capsule	98.5/94.3	43.1/55.9	61.1/91.3	98.9/98.3	77.1/97.3	91.1/98.6	76.0/73.3	76.0/73.3	96.7/96.6	97.0/99.1	69.8/60.9	86.2/80.1
	carpet	97.0/95.5	95.1/95.5	97.4/90.6	100/99.1	91.0/97.4	98.8/99.1	88.6/98.4	88.6/98.4	98.8/99.0	98.9/96.1	97.7/96.3	95.7/96.4
	grid	99.9/99.7	92.0/93.5	97.8/95.7	100/99.2	61.8/80.4	94.1/98.2	94.4/98.9	94.4/98.9	99.3/99.1	99.7/99.1	97.9/94.2	99.2/97.4
	hazelnut	100/99.7	91.9/93.5	98.8/94.9	100/99.1	99.8/97.9	100.0/99.0	99.5/98.5	99.5/98.5	100.0/99.0	99.9/99.6	100.0/87.6	100.0/97.6
	leather	100/98.6	99.9/96.2	99.0/96.9	100/99.5	100.0/99.3	100.0/99.2	99.9/99.4	99.9/99.4	100.0/99.1	100/99.7	95.1/98.2	100.0/99.6
	metal_nut	98.7/99.5	63.6/76.6	79.6/83.4	100/97.7	93.0/94.1	99.4/95.6	98.9/89.7	98.9/89.7	100.0/96.8	99.5/98.6	99.3/80.0	100.0/79.4
	pill	98.9/97.6	53.8/77.4	86.2/85.4	97.3/98.7	83.3/96.2	95.4/97.7	95.2/96.4	95.2/96.4	98.0/98.1	97.2/98.7	81.7/65.2	88.9/89.4
	screw	93.9/98.1	77.7/87.3	82.6/95.9	100/99.6	57.6/95.5	89.5/99.2	93.0/99.0	93.0/99.0	96.1/99.4	93.6/98.5	82.3/62.5	78.5/70.6
	tile	99.6/99.2	92.9/87.6	98.2/98.9	100/96.0	93.1/92.7	99.9/96.5	97.3/94.3	97.3/94.3	100.0/96.2	100/98.0	98.3/95.0	99.6/97.5
	transistor	93.1/90.9	82.5/92.7	90.0/92.6	98.7/95.4	91.9/97.2	97.2/99.0	100.0/98.7	100.0/98.7	97.8/99.1	98.5/89.1	73.6/92.1	83.3/95.7
	troothbrush	100/98.1	76.5/67.8	79.6/78.9	100/99.4	80.4/83.6	95.7/89.7	86.8/81.5	86.8/81.5	98.7/93.4	99.9/99.3	97.1/71.9	91.8/70.8
	wood	99.1/96.4	99.9/89.5	99.1/89.9	100/95.5	97.8/93.8	98.7/94.4	99.5/95.2	99.5/95.2	99.2/94.9	97.1/97.7	97.1/92.6	99.7/94.6
	zipper	100/98.8	93.6/87.3	96.8/82.6	99.6/98.3	89.3/97.4	99.4/98.0	99.4/98.6	99.4/98.6	99.6/98.3	100/99.1	98.4/91.2	99.5/87.5
VisA [22]	candle	92.8/86.3	78.1/72.0	86.0/97.0	88.7/97.4	81.1/97.1	91.8/99.2	94.2/99.1	94.2/99.1	96.9/99.7	96.2/89.6	85.4/70.9	87.7/80.9
	capsules	90.5/98.1	86.6/91.5	87.2/94.1	75.4/99.0	62.3/95.7	82.6/99.4	89.0/98.8	89.0/98.8	92.9/99.1	86.9/96.5	79.8/90.5	84.2/94.8
	cashew	97.1/81.6	95.5/62.4	96.7/91.5	91.8/97.9	84.6/94.4	88.7/93.7	81.7/99.1	81.7/99.1	86.1/99.4	94.2/96.3	84.5/77.6	86.1/87.2
	chewinggum	97.9/98.4	90.7/86.9	93.9/96.7	96.9/98.9	79.7/98.2	93.3/97.9	88.9/84.5	88.9/84.5	95.1/95.4	98.2/97.4	95.6/97.6	96.0/98.4
	fryum	95.4/93.8	78.3/78.0	85.9/84.3	95.6/96.4	82.5/96.0	95.2/96.3	90.0/96.6	90.0/96.6	97.6/98.5	88.6/89.2	91.7/69.4	90.2/73.6
	macaroni1	86.2/97.7	70.5/82.0	81.9/59.1	89.2/99.2	83.5/98.4	90.7/99.4	94.2/96.6	94.2/96.6	94.6/97.1	94.9/97.5	91.7/75.8	91.4/89.0
	macaroni2	85.4/96.4	65.2/91.3	45.6/90.7	79.4/99.1	53.6/97.4	79.3/99.3	94.6/99.7	94.6/99.7	93.6/99.7	80/92	63.2/68.0	71.3/74.1
	pcb1	92.4/93.5	68.3/85.4	91.4/95.1	98.4/99.4	55.8/98.0	95.1/99.5	82.2/99.5	82.2/99.5	83.9/99.4	96/94.6	88.9/95.9	88.7/97.9
	pcb2	95.3/96.0	77.2/89.3	93.2/97.4	97.2/98.8	93.7/97.0	94.8/98.5	97.1/97.6	97.1/97.6	97.2/98.9	96.5/95.4	91.0/92.7	92.2/97.6
	pcb3	94.0/89.7	88.1/87.3	92.8/97.5	98.4/98.7	58.6/96.3	95.9/98.9	95.0/97.6	95.0/97.6	95.3/98.8	97.8/94.1	92.5/89.8	94.6/92.4
	pcb4	96.5/88.0	97.3/92.6	98.4/96.3	99.9/96.1	98.9/94.5	99.8/98.6	99.8/97.1	99.8/97.1	100.0/98.3	99.5/92.4	98.8/88.4	98.6/95.9
	pipe_fryum	93.1/83.2	81.9/63.3	92.5/89.6	97.4/99.0	86.5/99.2	98.7/99.0	96.9/98.9	96.9/98.9	99.8/99.1	98.8/89.9	96.1/84.1	96.5/87.2
BTAD [13]	01	97.4/75.4	95.1/91.8	94.9/89.8	99.9/97.6	99.8/97.0	100.0/97.5	16.0/94.6	16.0/94.6	99.9/97.8	98.4/92.4	92.8/86.7	97.9/88.8
	02	80.3/82.1	73.1/76.1	75.9/90.4	86.4/95.2	76.0/96.0	87.9/95.7	84.4/97.0	84.4/97.0	87.1/96.5	84/92.9	85.7/91.3	86.2/88.5
	03	99.5/81	75.7/57.0	97.2/81.3	99.6/99.6	98.8/98.8	99.6/99.7	99.6/99.6	99.6/99.6	99.3/99.7	99.1/98.8	98.8/96.5	99.3/96.5
	total average	95.5/93.4	81.4/82.1	88.1/89.7	96.3/98.2	82.9/95.3	94.9/97.7	96.9/98.2	91.0/95.9	96.7/98.1	96.3/95.9	90.4/84.4	92.6/89.4